AWARD NUMBER: **W81XWH-12-1-0529**

TITLE: **Overcoming Autophagy to Induce Apoptosis in Castration-Resistant Prostate Cancer**

PRINCIPAL INVESTIGATOR: **Christopher Evans, MD**

CONTRACTING ORGANIZATION: **University of California, Davis**
Sacramento, CA 95817

REPORT DATE: **December 2016**

TYPE OF REPORT: **Final**

PREPARED FOR: **U.S. Army Medical Research and Materiel Command**
Fort Detrick, Maryland 21702-5012

REPORT DOCUMENTATION PAGE

Form Approved
OMB No. 0704-0188

1. REPORT DATE	2. REPORT TYPE	3. DATES COVERED
December 2016	Final	30Sep2012 - 29Sep2016

4. TITLE AND SUBTITLE

Overcoming Autophagy to Induce Apoptosis in Castration-Resistant Prostate Cancer

5a. CONTRACT NUMBER
W81XWH-12-1-0529

5b. GRANT NUMBER
PC111467

5c. PROGRAM ELEMENT NUMBER

6. AUTHOR(S)
Christopher P Evans, MD

E-Mail: cpevans@ucdavis.edu

5d. PROJECT NUMBER

5e. TASK NUMBER

5f. WORK UNIT NUMBER

7. PERFORMING ORGANIZATION NAME(S) AND ADDRESS(ES)

University of California, Davis
Department of Urology
4860 Y Street, Suite 3500
Sacramento, CA 95817-2307

8. PERFORMING ORGANIZATION REPORT NUMBER

9. SPONSORING / MONITORING AGENCY NAME(S) AND ADDRESS(ES)

U.S. Army Medical Research and Materiel Command
Fort Detrick, Maryland 21702-5012

10. SPONSOR/MONITOR'S ACRONYM(S)

11. SPONSOR/MONITOR'S REPORT NUMBER(S)

12. DISTRIBUTION / AVAILABILITY STATEMENT

Approved for Public Release; Distribution Unlimited

13. SUPPLEMENTARY NOTES

14. ABSTRACT

With the approval of the next generation anti-androgens such as enzalutamide and abiraterone (Abi) for advanced prostate cancer therapy, we attempted to evaluate whether combination of anti-androgen abiraterone and autophagy modulator metformin might block progression to castration resistant prostate cancer using the CWR22 xenograft model. CWR22 xenograft is considered the tumor model that may reprise tumor progression in patients under androgen deprivation therapy (ADT). CWR22 tumors normally reach around 100 mm3 in size in nude mice implanted with testosterone pellets in one month of time. After castration, tumors regress due to the decline of androgen and remain dormant for a length of time varying from 3 to 5 months. After that, tumors relapse and continue to grow vigorously independent of further ADT. However, due to the contamination of the frozen CWR22 samples used for tumor implantation, the assumed CWR22 tumors continued to grow after castration and were not inhibited by abiraterone, metformin and the combination.

15. SUBJECT TERMS

Castration resistant prostate cancer, autophagy, abiraterone, metformin, CWR22 xenograft, CWR22Rv1

16. SECURITY CLASSIFICATION OF:			17. LIMITATION OF ABSTRACT	18. NUMBER OF PAGES	19a. NAME OF RESPONSIBLE PERSON
a. REPORT	b. ABSTRACT	c. THIS PAGE			USAMRMC
Unclassified	Unclassified	Unclassified	UU	16	19b. TELEPHONE NUMBER *(include area code)*

Table of Contents

Introduction:

For our DOD award W81XWH-12-1-0529, we proposed to overcome autophagy as cell survival mechanism when treated with small molecule kinase inhibitor saracatinib or the androgen receptor signaling inhibitor enzalutamide in prostate cancer therapy. We started our study with saracatinib but had to switch to enzalutamide due to the halted effort by the pharmaceutical companies for the Src kinase inhibitors (AstraZeneca for saracatinib and BMS for dasatinib). Enzalutamide (Enza) is the new generation anti-androgen that has been approved by FDA for the advanced prostate cancer treatment. We have identified that enzalutamide elicits autophagy in castration resistant prostate cancer cell lines LNCaP C4-2B and LNCaP GRP cells. This treatment-mediated autophagy is through activation of AMPK and repression of mTOR [1-5]. Knocking down AMPK with siRNA reversed the survival mechanism and led cells to undergo apoptosis. Survival mechanisms elicited by CRPC C4-2B cells when treated with Enza may be blocked by inhibiting autophagy with clomipramine (CMI) [6, 7] and metformin (Metf) [8-10]. Combination of Enza with saracatinib and autophagy modulators significantly reduced cell proliferation in the LNCaP GRP CRPC model. Transcriptome deep sequencing of parental and Enza resistant C4-2B cells was carried out to examine differential gene expression pattern that may be related to their ability to survive under constant high exposure to ARSI. There were more than 140 genes up-regulated and more than 100 gene down-regulated, (3 FPKM = 1 transcript/cell). Figure 1 showed examples of up-regulated genes involved in autophagosome formation as expected in the ENZA resistant cells. Suppression of mTOR signaling is also a major inducer of autophagy. We observed several mTOR signaling genes that were differentially down-regulated in the resistant cells when compared to the parental cells (expression level are expressed in FPKM with 3 FPKM = 1 transcript/cell).

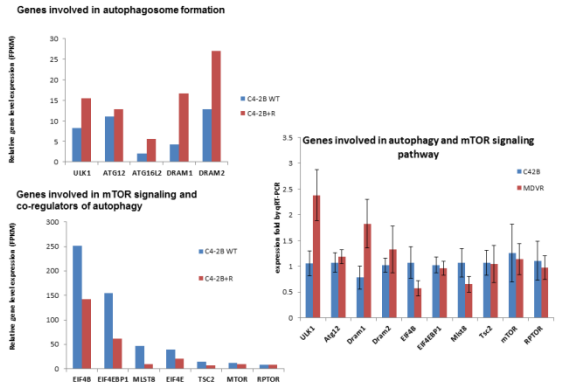

Figure 1. Transcriptome deep sequencing (left) of parental (WT) and enzalutamide resistant C4-2B (C4-2B+R) cells was carried out to examine differential gene expression pattern that may be related to their ability to survive under constant high exposure to ARSI. The data were validated with RT-qPCR (right).

in vivo studies using LNCaP C4-2B enza-resistant, GRP-Pro orthotopic and CWR22 xenograft models. With the former two CRPC models, combination of Enza with autophagy modulators CMI or Metf; or with saracatinib significantly reduced the tumor growth. The latter xenograft model showed that saracatinib alone may inhibit recurrence of castration resistant tumor growth after surgically castrated the CWR22 tumor bearing mice.

Keywords:
Castration resistant prostate cancer, autophagy, enzalutamide, CRPC animal models

Overall Project Summary:

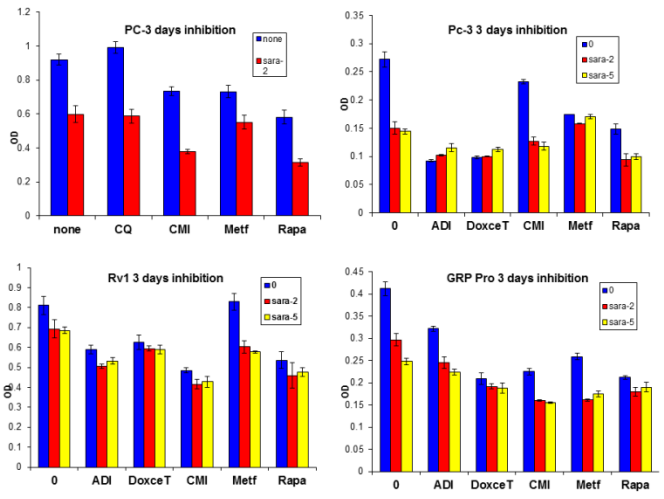

Figure 2. Cell proliferation under various treatments. Addition of autophagy modulators promoted cell killing by saracatinib alone.

Aim 1: To credential inhibition autophagy in conjunction with inhibition of Src, arginine or androgen receptor-axis pathways as a new therapeutic strategy

Major Task 1: Credential inhibition of Src and arginine pathways as a new therapeutic strategy

It was reported that when cells treated with the Src inhibitor saracatinib, they would be growth inhibition mainly through growth arrest but not apoptosis due to the autophagy survival pathway [5]. Apoptosis was promoted when the autophagy inhibitor cloroquine

(CQ) was added. We then tested more autophagy modulators such as clomipramine (CMI), metformin (Metf) and rapamycin (Rapa) on PC-3 cells. CQ did not show growth inhibition alone, whereas CMI, Metf and Rapa did. When combined with saracatinib, CMI and Rapa showed additive inhibition (figure 2). With a still broader experiment, PC-3, CWR22Rv1 and LNCaP GRP-Pro cells were treated with arginine deaminase inhibitor (ADI),docetaxol, CMI, Metf or Rapa alone or in combinations with saracatinib (2 or 5 μM). Each treatment alone displayed some inhibitory effect on cell proliferation and the degree varied from cell line to cell line. When combined with saracatinib, further cell killing was observed. Because of the lower toxicity and side effect of CMI (as an anti-depression drug) and Metf (as the diabetic drug) than CQ or Rapa, we decided to focus on the former two autophagy modulators in our studies.

Major Task 2: LNCaP C42B-MDV resistant cells, second CRPC model

We used LNCaP and CWR22Rv1 cells stably transfected with LC3-eGFP construct to investigate autophagy as the potential cell survival mechanism with anti-androgen treatments. Both cell lines were treated with 10μM of Enzalutamide, a new generation of antiandrogen drug through MTA with Medivation. LC3-I in cells is localized in the cytosol; but upon induction of autophagy, it is lapidated into LC3-II and inserted into autophagosome membrane and can readily be detected and visualized by the prominent change from diffuse cytoplasmic to bright, punctate fluorescence in the cytosol as shown in Figure 3A. Additional evidence of Enzalutamide-induced autophagy in LNCaP and CWR22rv1 cells came from Western blot analysis as demonstrated by the significant increase in the LC3-I to LC3-II conversion (LC3-II/I ratio increased from 0.71 to 1.36) and the increased expression of ATG 5, both have been used as reliable marker of autophagy (Figure 3B) [11]. Flow cytometry was also used to measure and quantify increase of autophagosome formation upon Enzalutamide treatment as shown in Figure 3C.

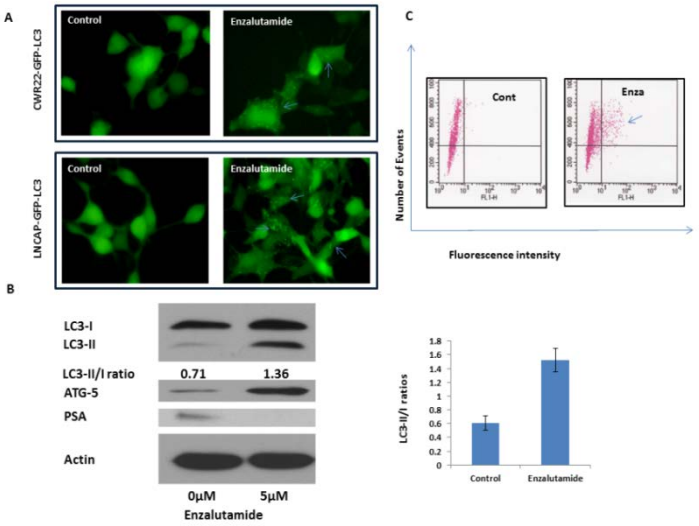

Figure 3. A. Representative fluorescence microscopy of CWR-22Rv1-eGFP-LC3 (upper panel) and LNCaP-eGFP-LC3 (lower panel) cells treated with DMSO (vehicle control), 10 μM Enzalutamide for 48 h viewed by fluorescence microscopy, showing GFP-LC3 localization and puncta autophagosome formation represented by arrow. B. C4-2B and LNCaP cells were treated with 5 μM Enzalutamide, and cell lysates were harvested and subjected to Western blotting analysis using autophagy markers, LC3-I and LC3-II and ATG-5. PSA was used as internal control. β-actin was used as the loading control. C. Upon induction of autophagy, autophagosomes formed in eGFP-LC3 transfected cells may be gated and numbered to report the degree of autophagy using flow cytometry.

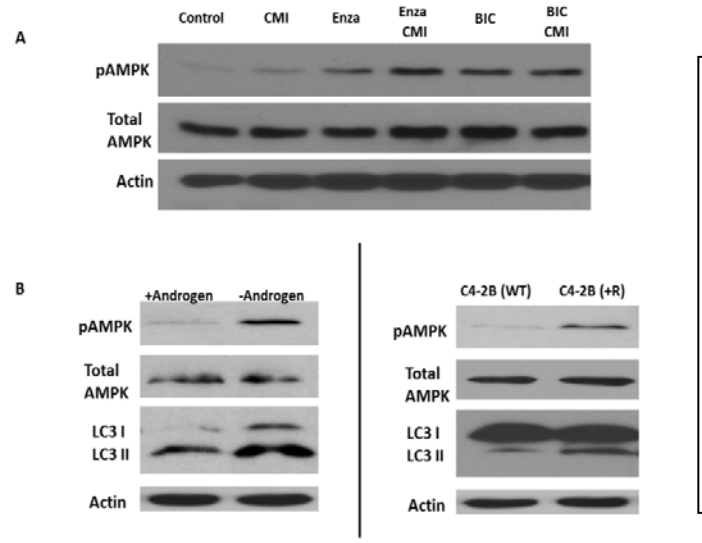

Figure 4 A. AMPK is activated with androgen receptor blockage. LNCaP and C4-2B cell lines were treated with DMSO (vehicle control), 5 μM CMI, 10 μM Enza, combination of CMI and Enzalutamide, 10μM biclutamide (Bic), combination of Bic and autophagy inhibitor CMI for 48 h. Cell lysates were harvested and subjected to Western blotting analysis using autophagy markers, LC3-I and LC3-II and antibodies to phospho AMPK and total AMPK. B. Androgen deprivation and continuous androgen blockage by Enzalutamide induces autophagy and activates AMPK phosphorylation. Left panel showed representative Western analysis of C4-2B cells cultured under regular FBS (+Androgen) and charcoal stripped FBS (-Androgen). Right panel showed similar analysis using Enzalutamide resistance cells (C4-2B +R) and their counterpart parental line (C4-2B -WT).

Because the AMPK activation has been implicated under androgen deprivation condition, we asked whether antiandrogen may activate this pathway, thereby inducing autophagy.[1].

To determine the predominate mechanism involved in androgen receptor signaling inhibitor (ARSI) mediated autophagy, we subjected C4-2B and LNCaP cells to both bicalutamide and Enzalutamide treatment and analyzed for phosphorylated AMPK and AKT. As shown in Figure 4A, activation of AMPK significantly increased in cells treated with ARSI, while the level of phosphorylated AKT is minimally affected (data not shown). We next evaluated AMPK phosphorylation in cells that conferred resistant to ARSI; namely C4-2B and C4-2B+R (C4-2B cells selected after prolonged enzalutamide exposure) cells. Under androgen deprivation (Figure 4B left panel) or prolonged androgen receptor blockage with Enzalutamide (right panel), the induction of autophagy was coupled with the activation AMPK, again suggesting that AMPK plays a crucial role in the induction of autophagy.

To prove the principle that activation of the AMPK pathway is responsible to the induction of autophagy mediated by ARSI, we used interference RNA to knock down the expression of AMPK in C4-2B cells and subsequently treated them with Enzalutamide. Autophagy was not observed in cells with diminished level of AMPK expression as evidenced by the lack of green fluorescence punctate, but can readily be detected and visualized by the prominent, bright punctate fluorescence in the cytosol of cells transfected with the scrambled control (Figure 5A). Previous studies demonstrated that the AMPK pathway directly interacts with TSC2/Raptor/mTOR complex to inhibit mTOR/S6K/4EBP signaling and the subsequent activation of autophagy [2, 12, 13].

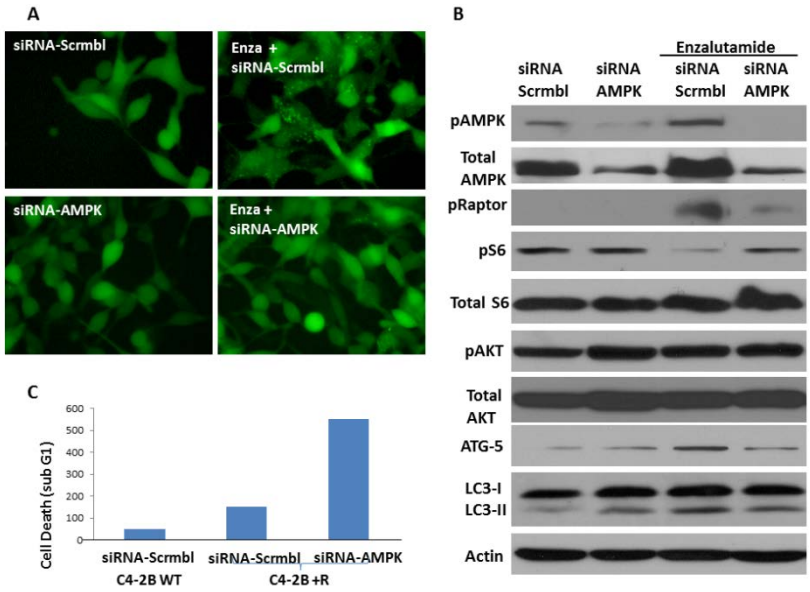

Figure 5 A. Knock down of AMPK in LNCAP-GFP cells blocks the induction of autophagy. LNCaP-eGFP-LC3 cells were transfected with negative control siRNA or siRNA targeting AMPK and treated with DMSO (vehicle control), 10 μM Enzalutamide for 48 h and were then analyzed by fluorescence microscopy. Shown are representative fluorescence microscopy of LNCaP-eGFP-LC3 showing GFP-LC3 localization and puncta autophagosome formation represented by arrow. B. Antiandrogen induced autophagy is mediated through activation of AMPK activation and inhibition of mTOR signaling via Raptor. C4-2B cells were transfected with negative control siRNA or siRNA targeting AMPK and treated with DMSO (vehicle control), 10 μM Enzalutamide for 72 h and cell lysates were analyzed by immunoblotting with antibodies as indicated. Controls were treated with vehicle alone. β-actin was detected as loading control. C. quantification of sub-G1 population in AMPK knock down cells 72 h after transfection.

Cells with knock down expression of AMPK were treated with vehicle and Enzalutamide, and then probed for phosphorylated Raptor, specifically detecting the phosphorylation of S792. As shown in Figure 4B, in the present of Enzalutamide and intact AMPK expression phosphorylated raptor level increased significantly, resulting in the consequential down regulation of pS6 and increased LC3-I to LC3-II conversion while pAKT remained unaffected.

When AMPK was effectively knocked down, Enzalutamide treatment did not affect the phospho-Raptor or phospho-S6 levels. These observations also correlated with reduced Atg-5 expression and reduced conversion of LC3-I to LC3-II. Hence, our data suggest the interaction between AMPK activation and suppression of mTOR via phosphorylation of Raptor at Serine 792 in the induction of ARSI mediated autophagy.

Figure 5C showed enhanced cell killing when AMPK was knocked down in the Enzalutamide resistant cells. The data support the notion that once the upstream signals for autophagy induction were suppressed, the

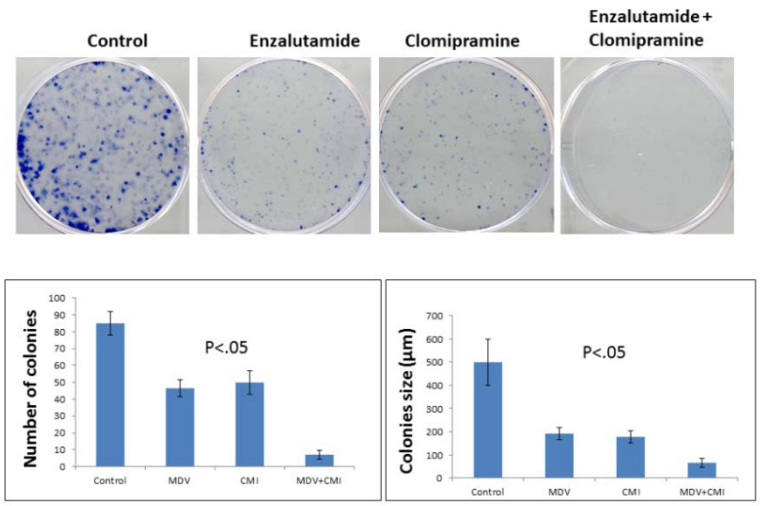

Figure 6. Blockage of antiandrogen-induced autophagy decreases cells' ability to form colonies. C4-2B cells treated with DMSO (vehicle control), 5µM CMI, 10µM Enza, combination of CMI and Enza, and used clonogenic assay to evaluate cells ability to form colonies. Left panels showed quantification of colonies number and colonies size. Significant difference between treatment groups were found using T-test ($P< 0.05$). Values represent mean ± SE.

Enzalutamide resistant cells become re-sensitized to ARSI induced cell-death. To provide an implication for therapeutic potential, we ask the question whether blocking autophagy would overcome Enzalutamide resistant in-vitro and in-vivo. Clonogenic assays were used to evaluate cell ability to form colonies in the present of an autophagy inhibitor Clomipramine (CMI). Clomipramine is an FDA approved drug to treat depression and has been shown to be a potent inhibitor of autophagy with little toxic affects both in-vitro and in-vivo [6, 7]. Colony formation in cells treated with Enzalutamide or CMI alone was slightly reduced compared to control, but was markedly impaired in the combined treatment. Their proliferative potential was also markedly reduced, based on the size of the colonies as shown in Figure 6. We will address our hypothesis that targeting autophagy could overcome resistant to Enzalutamide therapy in CRPC in an in-vivo Specific Aim 2: Application of inhibition of autophagy in combination with prostate cancer therapy in various CRPC and specific CaP disease states model next.

We further attempted to knock down two of the autophagy central molecules Beclin 1 and Atg5 to examine the effect of modulating autophagy in anti-androgen treatments. Real-time qPCR was performed to validate the deep sequencing data and found the trend agreeable. LNCaP LC3-GFP cells were transiently transfected with control (NTC), siRNA against beclin1 (Bcn1) or Atg5 [14], followed by treatments with DMSO, Enza, Metf or in combination. Cells became sensitized to Enza and even more to Enza+metf after the autophagy genes were knocked down (Figure 7). Less punctae formation was detected in the siBcn or siAtg5 cells when treated with Enza.

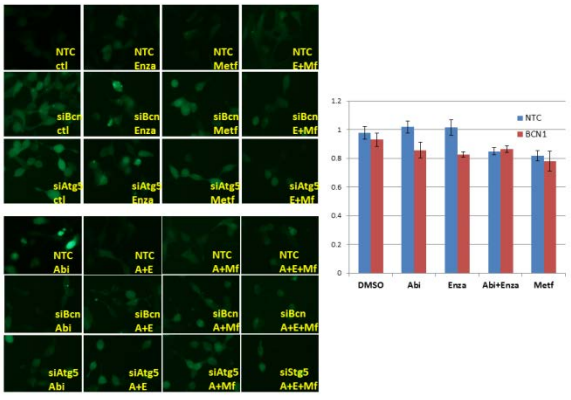

Figure 7. LNCaP LC3-GFP cells were transiently transfected with control (NTC), siRNA against beclin1 (Bcn) or Atg5, followed by treatments with DMSO, Enza, Metf, Abi or in combination. Autophagy represented by punctae of LC-3 was observed under fluorescence microscopy (left). MTT viability assay performed on the same setting showed the enhanced cell death after knocking out of Bcn1.

Metformin treatment on top of Enza further caused the morphology changes, cells were rounded up under the microscope indicating loss of viability. In additionally, they were treatments with abiraterone (Abi) or in combination with, Enza, Metf and both. Again, cells became sensitized to Abi and even more to combinations after the autophagy genes were knocked down. MTT assay was performed in C4-2B Enza-resistant cells with siRNA against beclin 1 followed by treatments with Abi, Enza, Metf or Abi+Enza. Anti-androgens alone did not inhibit growth in cells transfected with non-target control siRNA. However, cells with beclin1 knocked out became more susceptible to those drugs. Combination of Abi and Enza showed more potent effect even in the presence of autophagy pathway and so did metformin treatment. We are currently looking at the mechanisms behind.

Aim 2: Application of inhibition of autophagy in combination with prostate cancer therapy in various CRPC and specific CaP disease states

Testing the combination of enzalutamide and CMI (or metformin) on LNCaP C42B MDVR orthotopic mouse model

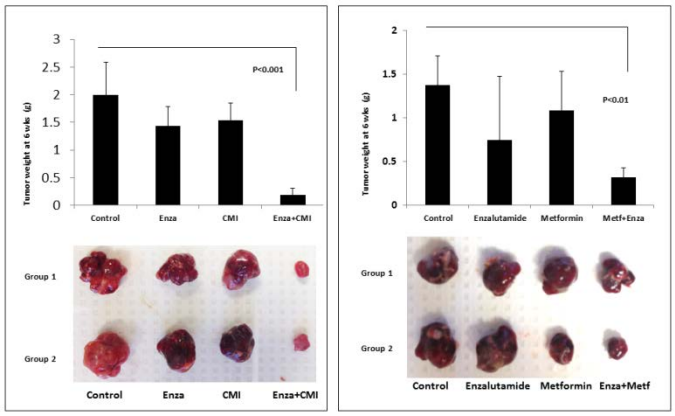

Figure 8. Two sets of orthotopic mouse studies were conducted with enzalutamide resistant C4-2B cells implanted into prostates of SCID mice. Drug treatments include enzalutamide, CMI, Metf or in combination. The graphs the average weight of tumors in each group, and two representative images of the tumors. Enzalutamide, clomipramine and metformin monotherapies did not inhibit the orthotopic tumor growth significantly. However, combination of Enza+CMI and Enza+Metf treatments significantly reduced tumor weights when compared to the control group.

To address our hypothesis that targeting autophagy could overcome resistant to ENZA therapy in CRPC in an in-vivo model, we used SCID mice and orthotopically implanted ENZA resistant cells into the prostate. PSA level was monitored until detectable around day 10, indicating tumor implantation. Treatments with control vehicles, CMI, ENZA and combination were dosed daily. At the end of six weeks from surgery, tumors were harvested and weighed. Mice treated with ENZA or CMI alone showed a 28% and 23% decrease in tumor size when compared control mice, respectively. There were a significant reduction in tumor size by 91% in mice treated with ENZA in combination with the autophagy inhibitor, CMI when compared to control mice, as shown in Figure 8 ($p<0.001$). Because the elevated interest of metformin also as an autophagy modulator and its low toxicity and applicability, we conducted another in vivo study replacing CMI with metformin. Mice treated with ENZA or metformin produced marginally reduced tumor sizes than the control mice, while those treated with the combination of ENZA and metformin gave a drastic 78% reduction with a significant difference ($p\leq0.01$ by Student's T test). Addition of metformin in the treatment also effectively blocked the autophagy survival mechanism tumor cells used when treated by anti-androgen enzalutamide. Tumors collected from different treatment groups, ctl, Enza, CMI and Enza+CMI were parafilm embedded and sectioned for H&E and immunohistochemical staining with antibodies against Ki67 or AR (Figure 9). H&E staining showed characteristics of prostate tumors; Ki67 demonstrated viability of cancer cells in tumors and AR nuclear localization or not reflected the drug effect of ARSI enzalutamide. The same analysis was performed for the metformin group (data not shown) and comparable results were observed. We took representative samples from this study and extracted total RNA for further analysis. It was observed that the genes involved in autophagosome formation were up-regulated while those in m-TOR signaling suppressed in the C4-2B enzalutamide resistant cells. Therefore, we performed real time PCR quantitation on those genes from tumor samples of the control and Enza (MDV) treated groups. Indeed, an up-regulation of the autophagy promoting genes and down-regulation of those in the mTOR pathway were observed (Figure 10, top panel). The levels of some AR downstream molecules and intracrine androgen synthetic enzymes were also examined (Figure 10, lower panel). Both PSA and TMPRSS2 levels decreased drastically with either enzalutamide or metformin alone. Two important enzymes in the backdoor androgen synthetic pathway, AKR1C3 and CYP17A1 were also greatly affected by all treatments.

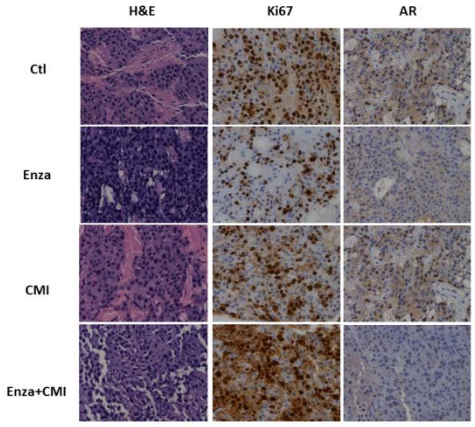

Figure 9. Tumors collected from different treatment groups, ctl, Enza, CMI and Enza+CMI were parafilm embeded and sectioned for H&E and immunohistochemical staining with antibodies against Ki67 or AR. The same analysis was done for the metformin group and got comparable results.

A scheme (Figure 11) summaries the interaction between AMPK mediated autophagy and mTOR signaling pathway. Metabolic stress including genotoxic stress, hypoxia, metformin treatment, Androgen deprivation ARSI treatment such as enzalutamide will activate AMPK and suppress mTOR that leads to autophagy.

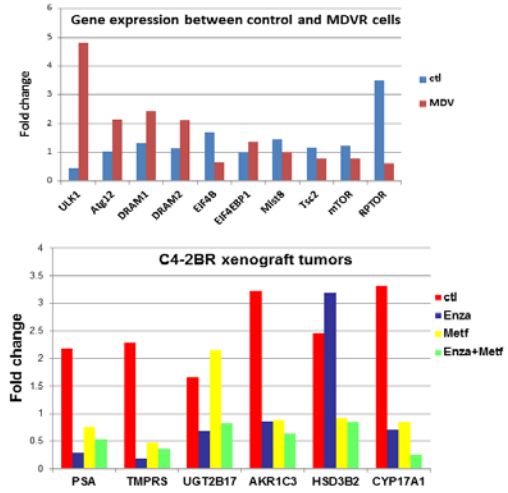

Figure 10. Total RNAs extracted from representative tumors from control, Enza (MDV), Metf and Enza+Metf groups were subjected to RT-qPCR for the genes indicated. Genes involved in autophagy pathways were compared between control and Enza (MDV) groups in the top pannel. Up-regulation of genes promoting autophagy was apparent. Genes regulated by AR signaling and those involved in androgen biosynthesis were shown in the lower panel. Most of the expression went down with just a single treatment and the combination ensured the low expression for all genes.

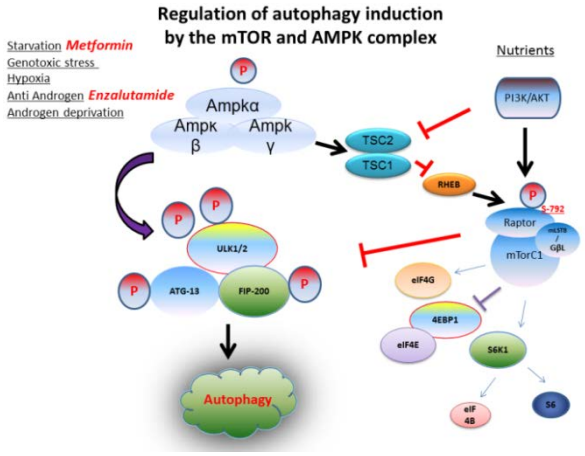

Figure 11. AMPK and mTOR pathways in response to the ARSI and other androgen deprivation treatment. Most of the molecules summarized here were flagged for up and down regulation in our deep sequencing analysis.

Major Task 3: Inhibtion of autophagy in a neuropeptide/Src mediated CRPC model

LNCaP GRP Pro cells had been characterized as CRPC cells. Growth of GRP Pro cells in androgen deprived environments was propelled by GRP mediated signaling pathway via Src kinase to activate androgen receptor (AR) in the absence of its cognate ligand [15]. Saracatinb was able to inhibit GRP Pro cell growth in vitro but not as significant in vivo. In addition to the ability of GRP Pro cells to synthesize intracrine androgen through up-regulating some crucial biosynthestic enzymes such as AKR1C3 and CYP11A, autophagy was considered the other contributing factor. We tested the two autophagy modulators CMI and Metf in combination with saracatinb on GRP Pro growth. Enzalutamide was also used with same dose of bicalutamide as a reference (Figure 12). Inhibiting Src kinase in GRP Pro cells rendered the CRPC cells more susceptible to anti-androgens such as bicalutamide and enzalutamide. Combining CMI and Metf with saracatinib also enhanced the cell killing. Metf also displayed some additive effect in inhibiting cell proliferation when combined with enzalutamide.

Using all three inhibitors, saracatinib, enzalutamide and metformin reduced cell growth to the lowest. The trends were observed in two independent set of experiments using either MTT assay or trypan blue cell counts.

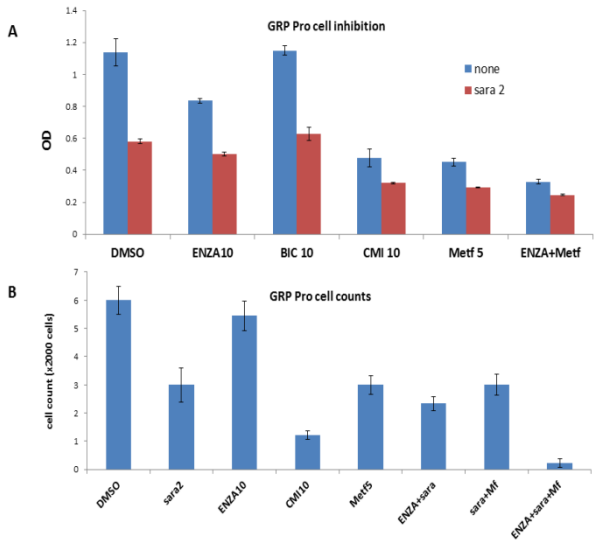

Figure 12. Cell proliferation inhibition by enzalutamide, bicalutamide, CMI, Metf alone or in combination with saracatinib, assayed by MTT or trypan blue cell counts.

Since enzalutamide is known to block AR nuclear translocation, we extrated cells treated with various reagents into nuclear and cytosolic fractions and separated them by SDS-PAGE, probed with different antibodies (Figure 13). When grown in regular media, GRP Pro cells were sensitive to enzalutamide, showing reduction of AR protein in the nuclear fraction.

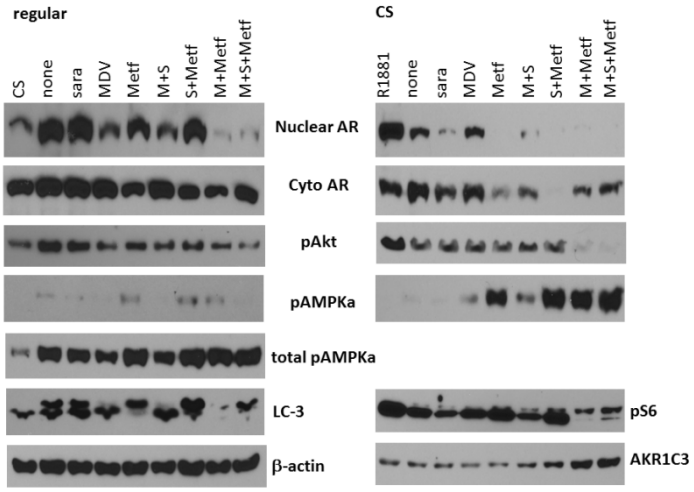

Figure 13. Western blotting analysis of LNCaP GRP-Pro cells grown in regular (left) or CS (right) media, treated with different single or combined inhibitors. AR distribution in the nuclear and cytosolic factions was examined. Autophagy status was suggested by transition of LC-3-I to LC-3-II and activation of AMPKa and S6.

Saracatinib showed no effect in this condition since AR was readily activated by its ligand. Metformin alone only decreased the AR translocation marginally. Yet, combination of enzalutamide and metformin almost totally blocked AR into nuclei. However, when in CS media, AR nuclear fraction was not affected by enzalutamide; whereas saracatinib reduced the nuclear translocation greatly which was in agreement with our previous observation [15]. Metformin treatment in CS conditions diminished nuclear AR almost to completion and also reduced cytosolic AR. The activation status of Akt decreased slightly in the regular serum condition but remained mostly unchanged except for enza+metf and enza+sara+metf. Activation of AMPKα and ribosomal S6 or transition from LC-3 I to II indicated autophagy.

For LNCaP GRP-Pro cell model, we have defined the rationale behind androgen-free cell proliferation was via neuropeptide GRP-mediate AR activation [15]. Src kinase was activated upon binding of GRP to its receptor on the cell surface. The phosphorylated Src simultaneously recruits and activates Etk and Fak and the three form Src-Etk-Fak complex to activate AR in the absence of ligand androgen. On the other hand, GRP-Pro cells demonstrated up-regulation of essential steroidogenic enzymes such as AKR1C3, HSD3B2, CYP17A1 and etc. Intratumor testosterone levels were detectable in GRP tumors developed in castrated mice [16]. With these known facts and in vitro study results, we hypothesized that the growth of CRPC GRP-Pro tumors in castrated animals would be inhibited when treated with both saracatinib and Enzalutamide. For the orthotopic tumor model, 32 male SCID mice were castrated and orthotopically injection with 2 x 10^6 LNCaP-Pro cells co-suspended in 30% matrigel (BD). Animals were randomly divided into 4 groups 2 weeks after surgery and subjected to daily dosing of buffer, saracatinib (25 mg/kg), Enzalutamide (10 mg/kg) or the combination for 5 weeks. Serum PSA was measured to ensure tumor take (Figure 14). GRP-Pro cells produced tumors in castrated male SCID mice in nearly all three treatment groups, control, sara and ENZA, with the combination treatment group, sara+ENZA only 5/8 tumor take rate. The mean tumor weight in the combination group was 37% of that from the control group (Figure 15). The two monotherapy groups showed no inhibition and even increased tumor weight in average. The PSA serum levels in the first three

Serum PSA ng/ml

control	saracatinib 25mg/kg	Enzalutamide 10mg/kg	sara+Enza	intact contol	castration control
40.87	44.04	234.64	28.28	198.19	7.41
200.15	214.45	264.57	60.28		
100.01	172.08	246.26	13.53		
187.23	163.25	5.52	5.35		
88.68	162.17	109.51	10.89		
197.89	112.51	26.25	5.33		
30.68	123.19	76.78	10.66		

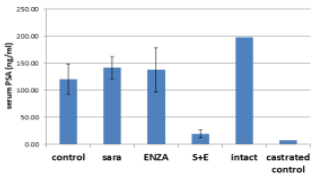

Figure 14. Serum samples were collected from castrated SCID mice orthotopically injected with LNCAP GRP-PRO cells. PSA levels were measured by a PSA ELISA kit (United Biotech). Serum samples from an intact mouse with LNCaP tumor and a castrated animal were used as the positive and negative references.

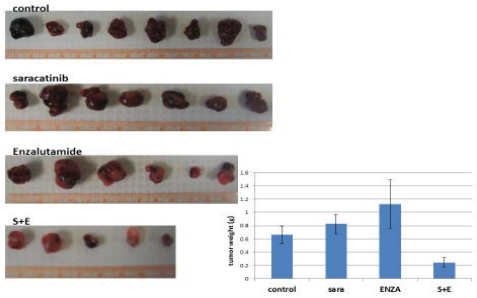

Figure 15. LNCaP GRP-Pro orthotopic tumors were harvested from castrated SCID mice. Tumor weight were measured and tallied, and the mean values of each group were graphed with standard errors.

groups were similar to that from an intact animal bearing prostate cancer tumors; whereas the combination group measured only 16% of the control. The immunohistochemical staining of representative samples clearly showed inhibition of pSrc by sara and inhibition of AR nuclear translocation in sara treated groups (Figure 16).

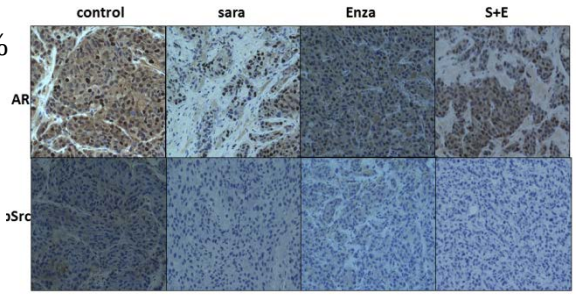

Figure 16. Tumor samples from each treatment groups were section and immunostained with anti-AR and anti-pSrc, respectively. Representative views are shown here.

Because of the specific driving force for the LNCaP GRP-Pro model, aberrant AR activation through neuropeptide (GRP) mediated signaling through the tyrosine kinases Src-Etk-Fak complex [15], the combination of saracatinib and enzalutamide was very effective in inhibiting tumor growth. Since autophagy mechanism is the focus of this funded project, we continued to test whether combination of autophagy modulator metformin with enzalutamide will also benefit the tumor treatment.

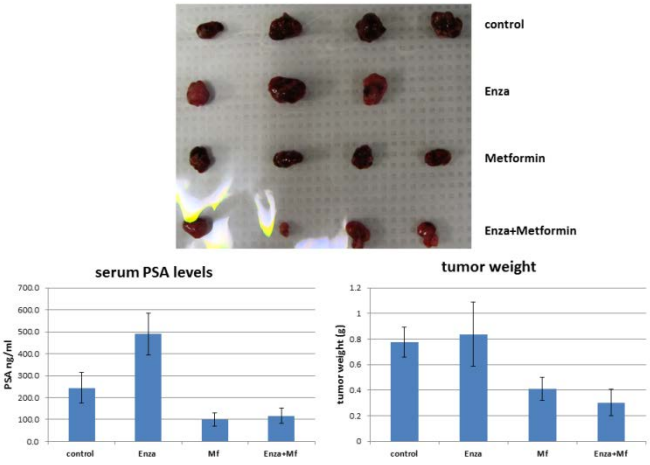

Figure 17. LNCaP GRP-Pro orthotopic tumors were harvested from castrated SCID mice. Serum PSA levels and tumor weight were measured and tallied, and the mean values of each group were graphed with standard errors.

Male SCID mice were castrated and orthotopically implanted with two millions of GRP-Pro cells. Serum PSA levels were measured 12 days later to confirm tumor take. Animals were randomly divided into 4 groups and treated with enzalutamide (25 mg/kg, p.o. daily), metformin (300 mg/kg, p.o. daily), combination or buffer only. After 30 days of treatments, animals were sacrificed. Blood and tumor were collected for analysis. The result (Figure 17) was consistent with previous findings that enzalutamide alone did not inhibit tumor growth. Serum PSA and tumor weight from the Enza group scored the highest among all. Metformin alone was powerful enough to bring down the serum PSA level and tumor weight by almost half. However, addition of enzalutamide with metformin did not completely abolish tumor growth. The benefit was minimal as the decrease in tumor weight from the combination group was only by 25% when compared to metformin alone. Decrease from neither group scored a *p* value for significant difference. This is probably due to the specific neuropeptide-mediated AR activation of the GRP-Pro line. Enzalutamide is never the ideal treatment drug. Although metformin may cause AR degradation, especially over the long-term treatment, AR activation via Src-Etk-Fak signaling is always present from GRP binding to its G protein-coupled receptor. The result of this model serves as an example for the need of precision medicine. If tyrosine kinase activation/up-regulation is the main force for the disease, a specific inhibitor to block that signaling pathway is required. The immunohistochemical staining of representative tumors from each group (Figure 18) showed that Ki67 decreased drastically in the Metf treatment, and so did in the Enza+Metf group. The AR staining was still prevalent in the Enza group but reduced profoundly in the Enza+Metf group.

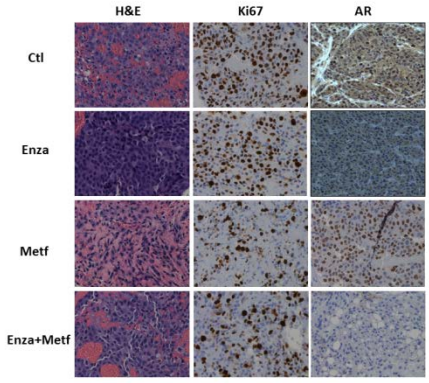

Figure 18. Tumor samples from each treatment groups were section and immunostained with antibodies against AR and Ki67, respectively. Representative views are shown here.

Major Task 4: Establish efficacy for combined inhibition of autophagy and tumor-specific pathwyas in specific CaP disease states

CWR22 xenograft model [17, 18] was used to mimic tumor recurrence after androgen deprivation therapy in patients. Athymic Nu/Nu male mice were implanted with CWR22 xenograft subcutaneously and allow for tumor progression. After tumor volume reached 100-150 mm^3, mice were surgically castrated and divided into groups, subjected to no treatment, treatments with saracatinib (25 mg/kg) or combined with chloroquine (50 mg/kg) from 7 days after surgery until 150 post-operation. CRPC recurrence was significantly inhibited with the administration of saracatinib. Mean of tumor recurrence (in tumor weight) for saracatinib, 0.18 grams and for control, 3.20 grams (p=0.015). Mean of serum PSA in the saracatinib-treatment group, 1.6 ng/ml and control, 14.7 ng/ml (P=0.08). The combination of saracatinib and chloroquine treatment did not show significant tumor suppression after recurrence. Therefore, only the control verse saracatinib treatment groups will be discussed here. We will repeat this experimental set-up but use metformin instead as a more reliable autophagy modulator. Tumor samples were collected at days 0, 30 and 150 (as summarized in the flow chart, Figure 19), total RNA was extracted for cDNA microarray analysis using Affymetrix Human Genome U133 Plus 2.0 chips. Heat maps (Figure 20) were generated and pathway analysis of gene differentially expressed in 150d control and saracatinib tumor samples was performed based on the gene profile. To give a couple of examples, the first heatmap showed averaged Cx-150d+AZD samples compared to averaged Cx-150Ctl ones: 2,582 genes differentially expressed 1,436 genes up-regulated 1,146 genes down-regulated. The saracatinib-response signature was determined by defining the common set of genes that were differentially-regulated by saracatinib in 2 different studies: CWR22 and A549. This signature of 520 probe sets was then used to perform unsupervised hierarchical clustering. The results suggest that a prominent component of the set of genes that were androgen-responsive and re-instated in the Cx-150d tumors were co-regulated by Src signaling shown in the second heatmap. The pathway analysis also showed that AR, CXCR4, MMP1 and a whole array of cell cycle genes such as CDC2, CDC20, CHEK1, RAD51 etc. may be the nodes in connecting pathways among molecules

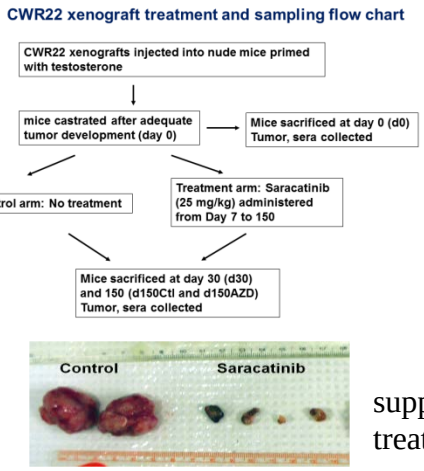

Figure 19. CWR22 xenograft treatment and sampling flow chart, with representing tumor samples from control and sara groups as the end of experiment.

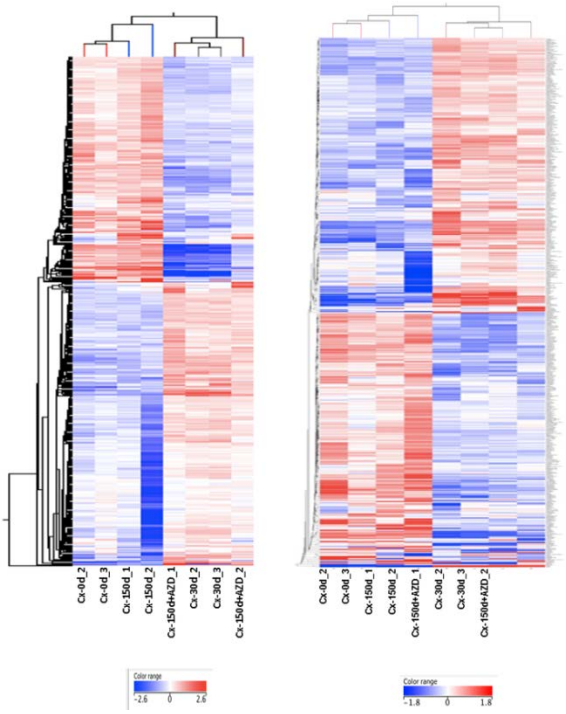

Figure 20. Two representative heatmaps generated from the gene profile for 150d control verses saracatinib (left) and saracatinib treated CWR22 xenograft verses A549 cells (right).

Table 1: Rank of changes in RNA expressions in CWR22 tumors from time points d30, d150Ctl and d150AZD with mean fold-change values represent the comparisons against d0 post-castration.

Gene Symbol	Fold change([D30] vs [D0])	Regulation([D30] vs [D0])	Fold change([D150_CTL] vs [D0])	Regulation([D150_CTL] vs [D0])	Fold change([D150_AZD] vs [D0])	Regulation([D150_AZD] vs [D0])
CORIN	33.75	up	2.58	up	40.52	up
UGT1A1,10 etc.	25.64	down	2.68	down	11.60	down
BIRC5	24.03	down	1.12	up	9.67	down
CDC2	16.41	down	1.16	up	8.05	down
LPL	12.67	down	5.88	down	7.94	down
CCNB1	12.41	down	1.14	up	5.33	down
AKAP12	12.20	down	1.22	down	12.58	down
PTTG1	11.63	down	1.05	up	7.23	down
BCHE	10.06	up	5.52	up	9.54	up
CDC6	9.83	down	1.60	up	5.24	down
ABCA1	9.81	up	1.85	up	6.35	up
BUB1B	9.31	down	1.08	up	6.09	down
MAD2L1	8.10	down	1.10	up	5.02	down
UBE2C	8.05	down	1.12	up	5.02	down
CXCR7	7.75	up	2.18	up	8.91	up
IQGAP2	7.25	down	1.02	up	5.13	down
MYBPC1	7.18	down	1.28	down	4.75	down
CDT1	6.48	down	1.18	up	4.63	down
MMP7	6.30	down	3.21	down	7.23	down
CDC45L	5.89	down	1.51	up	2.99	down
DDC	5.46	down	1.17	up	5.03	down
RACGAP1	4.86	down	1.15	up	3.46	down
ANXA3	4.65	up	1.44	up	5.68	up
IGFBP3	4.64	up	2.28	up	2.52	up
MCM4	4.52	down	1.45	up	2.59	down
CCNA2	4.44	down	1.27	up	3.23	down
PDK1	4.23	down	1.34	down	6.13	down
NR3C1	4.04	up	1.01	down	3.76	up
BRCA1	4.02	down	1.35	up	2.89	down
CEBPB	3.97	down	1.22	up	1.16	down

Table 2: Changes in RNA expressions of steroid biosynthesis/AR-regulated genes in CWR22 tumors from time points d0, d30, d150Ctl and d150AZD. Mean fold-change values represent the comparisons against d0 post-castration.

Gene Symbol	Fold change([D30] vs [D0])	Regulation([D30] vs [D0])	Fold change([D150_CTL] vs [D0])	Regulation([D150_CTL] vs [D0])	Fold change([D150_AZD] vs [D0])	Regulation([D150_AZD] vs [D0])
FASN	2.78	down	1.05	down	2.43	down
CYP11A1	1.01	down	1.02	up	1.12	up
CYP17A1	1.03	down	1.15	up	1.11	up
HSD3B2	1.08	up	1.02	down	1.08	down
HSD17B2	1.04	down	1.08	up	1.06	up
HSD17B3	1.56	up	1.10	up	1.66	up
HSD17B4	1.47	down	1.06	down	1.33	down
HSD17B10	1.47	down	1.16	up	1.42	down
AKR1C1	2.32	up	1.11	up	1.05	up
AKR1C2	1.91	up	1.11	up	1.07	up
AKR1C3	1.05	up	1.12	down	1.45	down
RDH5	1.11	down	1.16	up	1.17	down
SRD5A1	1.11	down	1.19	down	1.22	down
SRD5A2	1.11	up	1.04	up	1.10	up
SRD5A3	2.45	down	1.40	down	2.51	down
UGT2B15	18.79	up	2.21	up	12.98	up
UGT2B17	23.50	up	1.51	up	17.67	up
AMACR /// C1QTNF3	1.44	down	1.30	down	1.26	down
CYB5A	1.22	down	1.36	up	1.22	down
AR	2.41	up	2.21	up	1.69	up
EGR1	1.22	down	1.00	up	1.89	down
KLK3	1.04	down	1.10	down	1.09	up
TMPRSS2	1.21	down	1.28	down	1.04	down

Table 3: Changes in RNA expressions of pathway genes in CWR22 tumors from time points d0, d30, d150Ctl and d150AZD. Mean fold-change values represent the comparisons against d0 post-castration.

Gene Symbol	Fold change([D30] vs [D0])	Regulation([D30] vs [D0])	Fold change([D150_CTL] vs [D0])	Regulation([D150_CTL] vs [D0])	Fold change([D150_AZD] vs [D0])	Regulation([D150_AZD] vs [D0])
MYC	1.08	down	1.18	up	1.20	down
SRC	1.35	down	1.05	up	1.44	down
BMX	1.02	up	1.65	down	1.88	down
PTK2	1.77	down	1.14	up	1.36	down
CTNNB1	1.66	up	1.01	up	1.45	up
JAK1	2.25	up	1.21	up	2.26	up
JAK2	1.81	up	1.16	up	1.56	up
STAT3	1.10	up	1.10	down	1.10	up
NFKB1	1.04	down	1.18	up	1.14	up
NFKB2	1.27	up	1.14	up	1.15	up
AKT1	1.28	down	1.10	up	1.07	down
AKT2	1.03	down	1.16	up	1.08	down
AKT3	1.00	down	1.21	up	1.04	down
FRAP1	3.14	down	1.05	down	2.32	down
AURKA	9.73	down	1.03	down	5.35	down
AURKB	6.36	down	1.13	up	4.95	down

responding to castration, recurrence or Src kinase inhibition. From the microarray data, three groups of genes were tabulated and compared their response in the course of castration and treatments. The line-up of genes with the most change, either up or down-regulated was shown in the first table (Table 1). Steroid biosynthetic enzymes and AR regulated genes were grouped together (Table 2) and the third table showed genes involved in kinase activation. RT qPCR analysis was performed for selected genes of interest to validate the microarray data (data not shown).

We attempted to use the CWR22 xenograft model with combinational treatments of enzalutamide and abiraterone and autophagy modulator metformin last year. After almost 8 months of effort, we had to terminate the experiment because of lack of tumor relapse (Figure 21). Out of 42 mice, only 3 showed recurrence of tumor growth. We then tested different batches of CWR22 frozen xenograft on hand for a more aggressive inoculant for the subsequent experiment to conclude this funded study. With the more aggressive xenograft aliquots, we did not have to use testosterone pellet to initiate tumor take, which saved some supply expense to allow this repeated animal study.

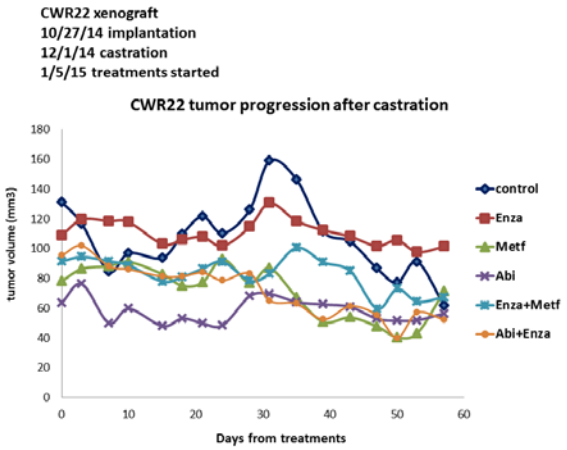

Figure 21. Tumor measurement of CWR22 xenograft mouse study after castration. Day 0 was the beginning of treatments, 35 days after castration when serum PSA levels receded to undetected. Tumor sizes eventually dwindled to nothing in almost all mice regardless of treatments.

We started with 48 male Athymoc nude mice, implanted with homogenized CWR22 tumor suspension subcutaneously. Less than 4 weeks later, most animals had developed reasonable size of tumors and were castrated surgically. Serum samples were harvested 2 days after castration and subjected to PSA ELISA assay. It was to our surprise that the serum PSA levels were very low, barely detectable (Figure 22). Normally, PSA levels in castrated mice started to decrease after castration but not at an abrupt rate. A good amount of PSA was still measurable from tumor-bearing mice 3 to 10 days after castration. According to our data, the magnitude of PSA in these mice 2 days post castration was only comparable to those 17 days post-op from a previous experiment. After some consideration, we decided to continue with the experiment with treatments: Abi (200 mg/kg/d, p.o.), metformin (300 mg/kg/d, p.o.) , the combination, or buffer alone. The humane end-point guideline was observed so animals were sacrificed when one dimension of the tumor was 20 mm. The tumor progression curves were

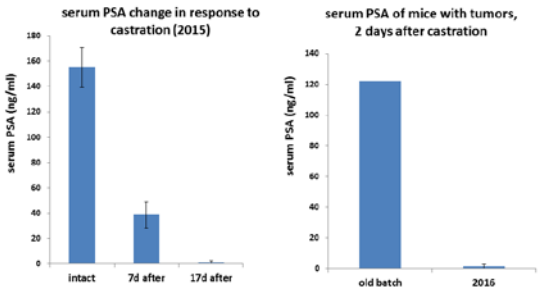

Figure 22. Serum PSA levels were measurement by PSA ELISA assay. Two sets of data, one from a previous experiment (left) and the other, current (right) indicate that abnormally low levels of PSA were in these tumor-bearing

plotted in Figure 23. The sharp decline of averaged tumor sizes was indication of early sacrifice of animals reaching the end-point. Overall, there was no statistical effect of drug treatments to tumor progression.

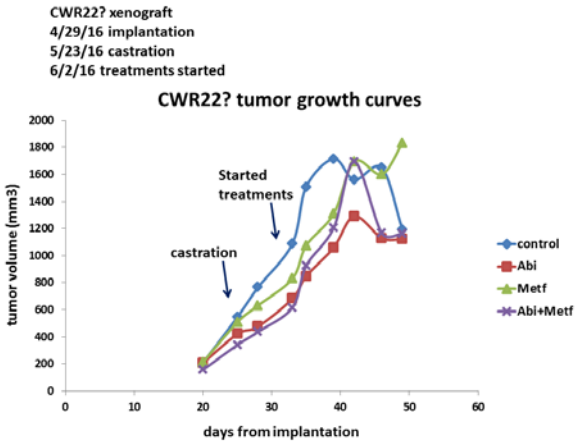

Figure 23. Tumor measurement of CWR22 (?) xenograft mouse study after castration. Day 0 was the tumor implantation, animals were castrated 25 days after and treated 35 days from the beginning. All tumor sizes continued to increase regardless of different treatments.

We harvested the tumors and performed Western blot analysis using specific antibodies to AR, PARP, ULK-1, AR-V7, cycline D1, p-S6, PSA and β-actin (Figure 24). All tumors appeared to contain very strong AR variants even when mice were intact. A majority of these variants were identified to be AR-V7, which should not be present in CWR22 xenografts grown in intact mice. The relapse variant of this xenograft, CWR22Rv1, has the reputation of containing high levels AR variants especially AR-V7. It was very likely that the inoculum contained Rv1 contamination. With C-terminal truncated AR present, the tumor would not be limited to activation by androgen. CWR22Rv1 tumors were known for expressing low levels of PSA. After castration, the intensity of full length AR decreased as expected. The levels of AR-V7 remained high in control and Abi groups but disappeared mostly in metformin treatment groups. This observation was in agreement with our previous finding that metformin caused AR/AR variants ubiquitination degradation. ULK-1 level reduced when mice were treated with metformin also suggesting that metformin was modulating, or inhibiting autophagy in this case. Some residual PSA was detected, indicating the tumor inoculum was not completely CWR22Rv1.

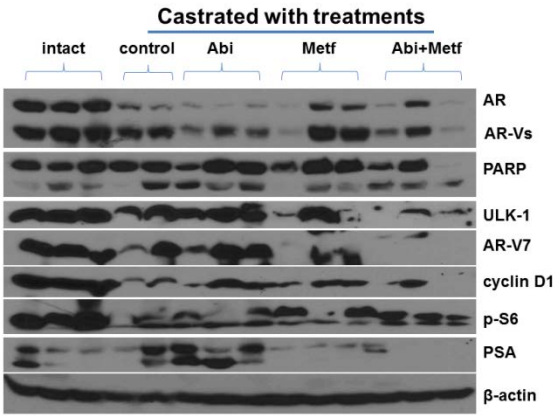

Figure 24. Western blotting analysis of tumor samples harvested at the end of experiment. Abnormally high amount of AR variants, especially AR-V7 suggested the tumor inoculum might have been contaminated with the relapse variant, CWR22Rv1.

Key Research Accomplishments:

1. Validated the additive effect of autophagy modulators on inhibition of cell proliferation to the kinase inhibitor and/or anti-androgen treatments.
2. Depicted the mechanism of anti-androgen mediated autophagy via the AMPK/mTOR signaling pathway in CRPC C4-2B cells, supported by in vivo studies and in depth analysis.
3. Demonstrated the effects of autophagy modulators on the CRPC LNCaP-GRP model both in cell proliferation and the autophagy and AR signaling axes. Combinatioin treatments of anti-androgne and kinase inhibitor and enzalutamide with metformin on the CRPC LNCaP-GRP in vivo model, target therapy may mechanistically block both neuropeptide and incracrine androgen mediated AR signaling axes. Results showed some effect of metformin in abrogating tumor growth. However, since enzalutamide could not strategically inhibit the CRPC growth of GPR-Pro cells mediated by neuropeptide-driven AR activation, coupling use of enzalutamide and metformin did not provide any treatment benefit for this particular case.
4. An in vivo study on molecules behind castration resistance using the CWR22 xenograft model.
5. Confirmed AR degradation caused by the metformin treatment in both C4-2B and GRP-Pro cells. The extent of degradation aggravated when metformin was combined with enzalutamide or abiraterone. This degradation was possibly mediated by E3 ligase Skp2. Detailed results were shown in the third year report.

Conclusion:

Survival mechanisms elicited by CRPC C4-2B cells when treated with Enza may be blocked by inhibiting autophagy with clomipramine and metformin. Combination of Enza with saracatinib and autophagy modulators

significantly reduced cell proliferation in the LNCaP GRP CRPC model. Further in vivo studies provided evidences to make autophagy targeting as a supplement to cancer therapeutic regimes. our studies to in vivo animal experiments. Three animal models, LNCaP C4-2B MDV-R, LNCaP GRP Pro cells and CWR22 xenograft were used. In LNCaP C4-2B MDV-R study, we validated that using autophagy modulators such as clomipramine and metformin, tumor survival mechanism encountering enzalutamide treatment may be blocked. A much significant reduction of tumor growth (91% and 78% for combinational use of CMI and metf with enzalutamide, respectively) was observed. In the LNCaP GRP model, combinational treatment of enzalutamide and saracatinib provided the best tumor suppression. Both specific mechanisms GRP cells utilizes for aberrant AR activation, intracrine androgen synthesis and kinase pathway mediated AR activation in the absence of androgen, were prevented through combined target therapy. As for the Enza+Metf combination treatment, anti-androgen enzalutamide alone is not the most effective therapy for this neuropeptide-mediated aberrant AR activation model. No tumor growth or PSA production was inhibited. On the other hand, metformin alone is able to sequester almost 50% of tumor growth. Combination did not add on much more effect. Lastly, castration resistant gene activation and tumor recurrence was inhibited by saracatinib treatment in the CWR22 xenograft model. We elected to use the CWR22 xenograft model to elucidate the role of autophagy in anti-androgen treatment of CRPC, with combinational use of autophagy modulator such as metformin. In the first attempt, a well-planned and exhausting effort of drug dosing was abated due to the failure of tumor recurrence after castration. Unfortunately, in the second try, there was contamination in our frozen xenograft deposit and we ended up using the likely CWR22Rv1 instead. With the full-grown Rv1 tumors, abiraterone or metformin combination treatment was not effective to control tumor growth even after castration. We have exhausted the fund and could not repeat the study any further. However, we were encouraged by the metformin effect on autophagy inhibition and AR/variant degradation and hopefully the combined enzalutamide and metformin clinical trial ongoing in our institute will have successful impact on CRPC patient treatments.

Publications, Abstacts, and Presentations:

Poster presentation:

1. Targeted Therapy using Saracatinib Adjunctive to Castration Inhibits Progression to Castration Resistant Prostate Cancer in a Murine Model. JC Yang, CG Tepper, B Hu, B Durbin-Johnson, AC. Gao, H-J Kung and CP Evans. AACR 2012
2. Enhanced in vivo inhibition of neuropeptide-mediated castration resistant prostate cancer progression by combination therapy with enzalutamide and saracatinib. JC Yang, HG Ngyuen, AC Gao, CP Evans. AACR 2013
3. Autophagy is a survival mechanism in mediating resistance to androgen receptor signaling inhibitors in castration resistant prostate cancer cells. HG Ngyuen, JC Yang, HJ Kung, AC Gao, CP Evans. AACR 2013
4. Targeting Autophagy Overcomes Enzalutamide Resistance in Castrate Resistant Prostate Cancer Cells and Improves Therapeutic Response in a Xenograft Model HG Nguyen, JC Yang, H-J Kung, XB Shi, D Tilki, RW deVere White, AC Gao and CP Evans AACR 2014
5. Metformin causes AR degradation via Skp2-mediated ubiquitination. JC Yang, AC Gao and CP Evans. AACR 2015.

Manuscript:

Targeting Autophagy Overcomes Enzalutamide Resistance in Castrate Resistant Prostate Cancer Cells and Improves Therapeutic Response in a Xenograft Model, HG Nguyen, JC Yang, HJ Kung, XB Shi, D Tilki, RW deVere White, AC Gao and CP Evans. *Oncogene* 2014. **33**(36): 4521-30.

Inventions, Patents and Licenses: N/A

Reportable Outcomes: N/A

Other Achievements: N/A

References:

1. Chhipa, R.R., Y. Wu, and C. Ip, *AMPK-mediated autophagy is a survival mechanism in androgen-dependent prostate cancer cells subjected to androgen deprivation and hypoxia.* Cell Signal, 2011. **23**(9): p. 1466-72.
2. Gwinn, D.M., et al., *AMPK phosphorylation of raptor mediates a metabolic checkpoint.* Mol Cell, 2008. **30**(2): p. 214-26.
3. Kim, J., et al., *AMPK and mTOR regulate autophagy through direct phosphorylation of Ulk1.* Nat Cell Biol, 2011. **13**(2): p. 132-41.
4. Nguyen, H.G., et al., *Targeting autophagy overcomes Enzalutamide resistance in castration-resistant prostate cancer cells and improves therapeutic response in a xenograft model.* Oncogene, 2014. **33**(36): p. 4521-30.
5. Wu, Z., et al., *Autophagy Blockade Sensitizes Prostate Cancer Cells towards Src Family Kinase Inhibitors.* Genes Cancer, 2010. **1**(1): p. 40-9.
6. Gillman, P.K., *Tricyclic antidepressant pharmacology and therapeutic drug interactions updated.* Br J Pharmacol, 2007. **151**(6): p. 737-48.
7. Rossi, M., et al., *Desmethylclomipramine induces the accumulation of autophagy markers by blocking autophagic flux.* J Cell Sci, 2009. **122**(Pt 18): p. 3330-9.
8. Ben Sahra, I., et al., *Targeting cancer cell metabolism: the combination of metformin and 2-deoxyglucose induces p53-dependent apoptosis in prostate cancer cells.* Cancer Res, 2010. **70**(6): p. 2465-75.
9. Ben Sahra, I., et al., *Metformin in cancer therapy: a new perspective for an old antidiabetic drug?* Mol Cancer Ther, 2010. **9**(5): p. 1092-9.
10. Ben Sahra, I., J.F. Tanti, and F. Bost, *The combination of metformin and 2-deoxyglucose inhibits autophagy and induces AMPK-dependent apoptosis in prostate cancer cells.* Autophagy, 2010. **6**(5): p. 670-1.
11. Klionsky, D.J., et al., *Guidelines for the use and interpretation of assays for monitoring autophagy.* Autophagy, 2012. **8**(4): p. 445-544.
12. Lee, J.W., et al., *The association of AMPK with ULK1 regulates autophagy.* PLoS One, 2010. **5**(11): p. e15394.
13. Inoki, K., T. Zhu, and K.L. Guan, *TSC2 mediates cellular energy response to control cell growth and survival.* Cell, 2003. **115**(5): p. 577-90.
14. Selvakumaran, M., et al., *Autophagy inhibition sensitizes colon cancer cells to antiangiogenic and cytotoxic therapy.* Clin Cancer Res, 2013. **19**(11): p. 2995-3007.
15. Yang, J.C., et al., *Aberrant activation of androgen receptor in a new neuropeptide-autocrine model of androgen-insensitive prostate cancer.* Cancer Res, 2009. **69**(1): p. 151-60.
16. Chun, J.Y., et al., *Interleukin-6 regulates androgen synthesis in prostate cancer cells.* Clin Cancer Res, 2009. **15**(15): p. 4815-22.
17. Nagabhushan, M., et al., *CWR22: the first human prostate cancer xenograft with strongly androgen-dependent and relapsed strains both in vivo and in soft agar.* Cancer Res, 1996. **56**(13): p. 3042-6.
18. Pretlow, T.G., et al., *Xenografts of primary human prostatic carcinoma.* J Natl Cancer Inst, 1993. **85**(5): p. 394-8.

Appendices: N/A